PASSIVE BISTATIC SAR IMAGING AND INTERFEROMETRY BY SATELLITE DIGITAL TV SIGNAL

[1]*Weike Feng,* [2]*Jean-Michel Friedt,* [3]*Giovanni Nico,* [2]*Gilles Martin,* [4]*Motoyuki Sato*

[1]Graduate School of Environmental Studies, Tohoku University, Sendai, Japan
[2]FEMTO-ST, Time & Frequency department, Besancon, France
[3]Consiglio Nazionale delle Ricerche, Istituto per le Applicazioni del Calcolo, Bari, Italy
[4]Center for Northeast Asian Studies, Tohoku University, Sendai, Japan

***Abstract*—In this study, we used the digital television signal broadcasted by geostationary satellite for passive bistatic synthetic aperture radar (SAR) imaging and interferometry applications. A prototype system was designed and fabricated with commercial-off-the-shelf (COTS) components. Specifically, three low noise block downconverters (LNBs) were synchronized for a long-time coherent measurement. Moreover, multiple TV channels were combined to achieve a wider frequency bandwidth to improve the range resolution. The potential applications of this ground-based radar system are SAR imaging, displacement estimation, and digital elevation model (DEM) generation. Hardware design and data processing algorithms are described. Experimental results are presented to validate the performance of the designed system and the proposed methods.**

***Index Terms*—Passive bistatic radar (PBR), Satellite digital TV signal, Synthetic aperture radar (SAR), SAR interferometry.**

I. INTRODUCTION

Recently, passive bistatic radar that uses existing broadcasting signals, communication signals, and navigation signals has drawn a lot of interests [1-2]. Compared to other illuminators of opportunity, such as WiFi and terrestrial TV signal, PBR using satellite digital TV signal has several advantages, including: 1) one TV channel can provide a frequency bandwidth larger than 30 MHz; if multiple TV channels are combined, a bandwidth larger than 150 MHz and thus a sub-meter range resolution can be obtained; 2) since its working frequency is at Ku band, a high-resolution change detection capability via interferometry technique can be achieved, like that in ground-based SAR [3-4]; 3) a larger illumination area and a clearer reference signal increase the usability and performance of the PBR system. For example, digital TV broadcasting with Broadcasting Satellite (BS) on the geostationary orbit of 110 degrees East longitude (BS 110°E) can provide services for the whole area of Japan.

However, there are also some difficulties when using the satellite TV signal for PBR applications, including: 1) the power density of the satellite TV signal on the Earth surface is normally much lower than some other signals used for PBR applications, such as FM and DAB, resulting in a lower signal to noise ratio (SNR) and a shorter detection range; 2) if some commercial-off-the-shelf (COTS) components are used to reduce the system cost, some modifications must be conducted to synchronize both frequency and phase between the reference channel and the surveillance channels for long-time coherent measurement; 3) the waveform of the digital TV signal is not designed for radar applications, its signal structure, including spectrum properties, pilot signals, and guard intervals, will introduce undesired artifacts in the range direction when the classical cross-correlation processing method is used; 4) when multiple frequency bands were combined to increase the range resolution, frequency gaps among different TV channels cause high-level artifacts in the range direction [5].

To solve these problems, we proposed a hardware design method and several processing algorithms in this paper. Firstly, we describe an LNB synchronization method to increase the integration time for SNR improvement. Secondly, we use the inverse filter technique to reduce the influence of the TV signal structure. Thirdly, we apply the super spatially variant apodization (Super-SVA) method to fill the frequency gaps among multiple TV channels to suppress the artifacts. Finally, based on a PBR prototype system using COTS components, SAR imaging and displacement estimation experiments are carried out to validate the proposed methods.

II. DESIGNED SYSTEM OVERVIEW

A. Adopted ISDB-S signal

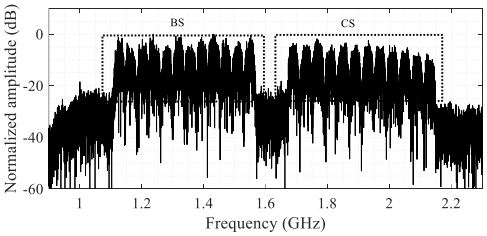

Fig. 1. The spectrum of the satellite TV signal in Japan.

The spectrum of the used satellite TV signal is shown in Fig. 1, where the local oscillator frequency of LNB is about 10.601 GHz. BS and communication satellite (CS) signals are broadcast by different satellites that are on the geostationary orbit of 110 degrees East longitude (110°E). Each TV channel has a frequency bandwidth of 34.5 MHz. If twelve channels of BS or CS are combined, a 475.5 MHz frequency bandwidth can be achieved, resulting in a maximal bistatic range resolution of 0.32 m. We note that, in this study, only CS signal is used for simplicity. BS signal transmitted via both left-hand and right-

hand circular polarizations will be used for multi-polarization applications in the near future.

B. Designed radar system

The designed radar system is shown in Fig. 2. It has three parallel receiving channels, one reference channel and two surveillance channels. For reference channel, a 45-cm parabolic antenna is used, while only the feed-horns of parabolic antennas are used for the surveillance channels to achieve a wider beam-width. Three LNBs with a local frequency of 10.601 GHz are synchronized by an oscillator controller. To further amplify the received signal, three COTS BS/CS boosters were used, whose working frequency is from 10 to 2600 MHz and gain is from 26 to 34 dB adjustable. Surveillance antennas are mounted on a positioner to generate a synthetic aperture with a fixed step in the horizontal direction. The signal flow will be sampled by a digital storage oscilloscope with a sampling frequency of 10 GHz. Finally, the acquired raw data are transferred to a local PC for off-line signal processing, consisting in frequency gaps filling, SAR imaging, and interferometric processing.

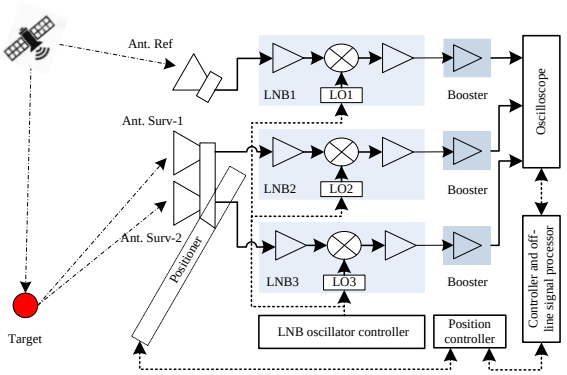

Fig. 2. The designed PBR system using satellite TV signal.

C. LNB synchronization

Since COTS LNBs have different local oscillators, their phase differences will reduce the coherence of the three receiving channels. When the data are sampled in a short time, the phase difference is approximately caused by their local frequencies only. Thus, a simple phase difference estimation method can be used [5], consisting in: 1) Divide the signal into U short-length (T) subsets, within which the phase difference is assumed to be constant, *i.e.*, f_1t and f_2t, where t=[0, T, ... , (U-1)T], f_1 and f_2 are the frequency differences between the surveillance LNBs and the reference LNB; 2) Do cross-correlation between the co-located reference and surveillance antennas to obtain the phase of peaks in each subset, which gives $e^{-j2\pi f_1 t}$ and $e^{-j2\pi f_2 t}$; 3) Finally, do Fourier transform of the peak phases, providing us with f_1 and f_2.

However, since SAR imaging and interferometric processes are desired and a longer integration time can increase the SNR and increase the detection distance, coarse phase correction is not enough. Thus, an advanced LNB synchronization approach is further proposed, whose setup is shown in Fig. 3. Based on the unpublished NXP application note "X-tal driver for using multiple TFF10xx to the same X-tal as reference" describing the mechanism for locking multiple TFF10xx PLLs on the same reference as desired, a dedicated Pierce oscillator was built around a 25 MHz resonator and a 74HC04 inverter. The output of the Pierce oscillator feeds another 74HC04 used to generate three sets of in-phase and phase-opposition (180-degree phase shift) signals feeding the PLL inputs. Care must be taken on the one hand to tune the output voltage amplitude to acceptable levels (500 mVpp) using a voltage divider bridge, and on the other hand to include a DC-blocking capacitor (5.6 nF) between the oscillator output and the PLL to avoid DC-current leakage from the PLL, which would prevent PLL locking. Under the proper conditions, frequency/phase coherence was observed to be stable over tens of minutes, as needed for SAR measurement.

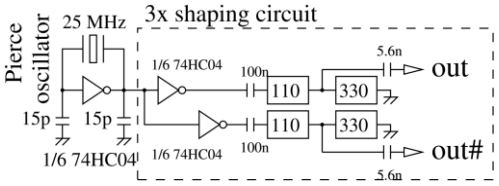

Fig. 3. LNB synchronization setup.

III. Inverse Filter and Frequency Gap Filling

A. Cross-correlation and inverse filter

Normally, a cross-correlation method is used to estimate the delay of the target, given by

$$\chi_a(\tau) = \int_0^{T_{int}} s_{sur}^a(t) s_{ref}^*(t-\tau)dt \tag{1}$$

which can be implemented by Fast Fourier Transform, giving

$$\boldsymbol{\chi}_a = \boldsymbol{\Phi}^H \boldsymbol{s}(\boldsymbol{f}) = \boldsymbol{\Phi}^H [\boldsymbol{s}_{sur}^a(\boldsymbol{f}) \odot \boldsymbol{s}_{ref}(\boldsymbol{f})^*] \tag{2}$$

where $s_{ref}(t)$ is reference signal, $s_{sur}(t)$ is surveillance signal, a = 1 or 2 denotes the first or the second surveillance channel, $(\cdot)^*$ denotes the complex conjugate, $\chi(\tau)$ is the range-compression result, τ is the expected time delay of the target, T_{int} is the integration time, $\boldsymbol{\Phi}$ is the Fourier transform matrix, $\odot$ denotes element-wise multiplication, $\boldsymbol{s}_{ref}(\boldsymbol{f})$ and $\boldsymbol{s}_{sur}(\boldsymbol{f})$ are the frequency domain signals of the reference and surveillance channels.

However, since the waveform of satellite TV signal is not designed for radar applications, the cross-correlation processing will introduce high-level artifacts in the estimation. A simple but effective method to solve this problem is to use an inverse filter to avoid the influence of the signal structure of the TV signal, which can be expressed as

$$\boldsymbol{\chi}_a = \boldsymbol{\Phi}^H \boldsymbol{s}_a^{'}(\boldsymbol{f}) = \boldsymbol{\Phi}^H [\boldsymbol{s}_{sur}^a(\boldsymbol{f}) \odot \boldsymbol{s}_{ref}(\boldsymbol{f})^* / |\boldsymbol{s}_{ref}(\boldsymbol{f})|^2] \tag{3}$$

B. Frequency gap filling

To improve the range resolution, multiple TV channels can be combined to obtain a wider bandwidth. However, different TV channels are separated by frequency gaps to guarantee a high-quality signal transmission, introducing artifacts into the range compression result. Several spectral gaps filling methods can be used, such as auto-regressive (AR) based method, Super-SVA based method, and sparsity and low-rank property based methods [5]. In this paper, Super-SVA method is used for its simplicity and effectiveness. Based on the SVA algorithm, the range compression result of the n-th (n = 1, 2,...,12) TV channel is given by

$$\boldsymbol{\chi}_{a,n}^{SVA} = \boldsymbol{\Phi}_n^H [\boldsymbol{s}_{a,n}^{'}(\boldsymbol{f}) \odot \boldsymbol{W}(\boldsymbol{f})] \tag{4}$$

where $\boldsymbol{W}(\boldsymbol{f})$ is a nonlinear "cosine on pedestal" weighting function that can be expressed as

$$W(m) = 1 - 2\beta\cos(2\pi m / M), \quad 0 \le \beta \le 0.5 \tag{5}$$

Then, the frequency gaps can be filled by Super-SVA via the following steps:

1) Perform Fourier transform of $\boldsymbol{\chi}_{a,n}^{SVA}$ to get $\boldsymbol{\chi}_{a,n}^{SVA}(\boldsymbol{f})$;

2) Apply an inverse weighting vector $W_{inv}(\boldsymbol{f})$ to obtain $\boldsymbol{s}_{a,n}^{S-SVA}(\boldsymbol{f}) = \boldsymbol{\chi}_{a,n}^{SVA}(\boldsymbol{f}) / W_{inv}(\boldsymbol{f})$;

3) Replace the center portion of the extrapolated signal $\boldsymbol{s}_{a,n}^{S-SVA}(\boldsymbol{f})$ with the original signal $\boldsymbol{s}_{a,n}^{'}(\boldsymbol{f})$.

According to this procedure, the gapped signal can be reconstructed for each TV channel. Since two adjacent channels have the same gapped frequencies, a simple average process can be used to obtain the final estimation. Finally, the range compression can be obtained by $\boldsymbol{\chi}_a^{S-SVA} = \boldsymbol{\Phi}^H \boldsymbol{s}_a^{S-SVA}(\boldsymbol{f})$.

IV. SAR IMAGING AND INTERFEROMETRY

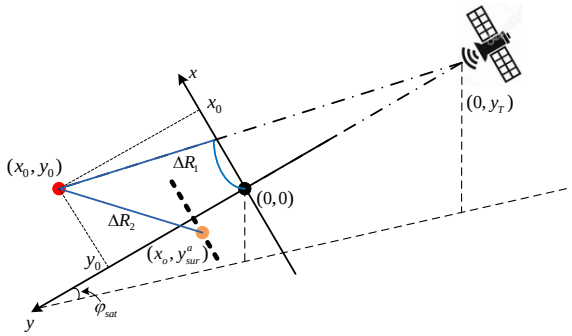

Fig. 4. SAR imaging geometry.

The imaging geometry of the designed radar system is shown in Fig. 4, where the reference antenna is located at (0, 0) and the surveillance antenna is scanned along a rail from $(-L/2, y_{sur}^a)$ to $(L/2, y_{sur}^a)$ with L as the synthetic aperture length. The elevation angle of the satellite is $\varphi_{sat} = 35.3^\circ$ in Sendai (Japan) area. For the o-th (o=1, 2,..., O) surveillance antenna position, the range compression can be conducted by applying Fourier transform to the gap filled signal, giving $\boldsymbol{\chi}_{a,o}^{S-SVA} = \boldsymbol{\Phi}^H \boldsymbol{s}_{a,o}^{S-SVA}(\boldsymbol{f})$. Then, the SAR image of the target can be obtained by applying the back projection (BP) algorithm, giving

$$\alpha_a(x,y) = \sum_{o=1}^{O} \boldsymbol{\chi}_{a,o}^{S-SVA}[\Delta R_1 + \Delta R_2^a(o)] \tag{6}$$

where $\alpha_a(x,y)$ is the estimated amplitude of the point at (x, y), ΔR_1 is the path difference between the TV satellite to the target and to the reference antenna, $\Delta R_2^a(o) = \sqrt{(x-x_o)^2 + (y-y_{sur}^a)^2}$ is the distance from the target to the o-th antenna position of the a-th surveillance antenna, and $\boldsymbol{\chi}_{a,o}^{S-SVA}[\Delta R_1 + \Delta R_2^a(o)]$ can be calculated by the linear interpolation process. Since the satellite is far from the experiment position, *i.e.*, $|y_T|$ is much bigger than x and y, ΔR_1 can be approximately calculated by

$$\Delta R_1 = \sqrt{x^2 + (y - y_T)^2} - |y_T| \simeq y \tag{7}$$

The designed passive radar system can acquire a time series of 2D SAR images of the scene with a temporal baseline of few minutes as the used geostationary satellite is continuously illuminating the area of interest. This allows many interesting interferometric SAR applications. For each pair of SAR images, an interferometric phase image can be generated by

$$\Delta\varphi_{D\text{-}In}(x,y) = \arg\{\alpha_{mater}^{*}(x,y) \cdot \alpha_{slave}(x,y)\} \tag{8}$$

As an application, the displacement of a target can be estimated by the relationship $D = \lambda\Delta\varphi_{D\text{-}In}(x,y)/4\pi$, where λ is the wavelength, which is 24 mm for the CS signal. Besides, we note that, since two surveillance antennas can be used, the developed system can also generate a high resolution Digital Elevation Model (DEM) of the imaging scene by properly setting a spatial baseline between the two surveillance antennas. DEM generation experiments are on-going and will be further researched.

V. EXPERIMENT RESULTS

In this section, some experimental results will be shown to validate the designed radar system and the proposed processing methodologies. At the beginning, a time delay estimation experiment using the satellite TV signal was conducted, as shown in Fig. 5, where two parabolic antennas with synchronized LNBs were faced toward the CS 110°E satellite. Twelve TV channels were combined and inverse filter is used for range compression. The estimation results are shown in Fig. 6, where two different integration times are assessed. As we can see, by increasing the integration time from 1 μs to 100 μs, the SNR can be increased about 10 dB, which proves that the LNBs are well synchronized. Otherwise, the SNR will not be increased but decreased because the two receiving channels are not coherent [5].

Fig. 5. Time delay estimation experiment setup.

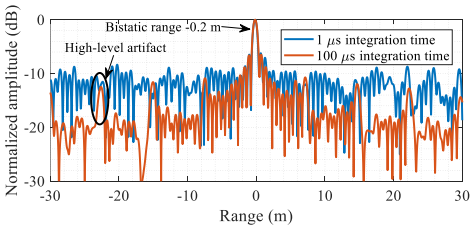

Fig. 6. Delay estimation results with different integration time.

However, as indicated by the black circle in Fig. 6, high-level periodical artifacts will be generated by the frequency gaps. By applying Super-SVA based frequency gap filling method, these artifacts can be well suppressed, as shown in Fig. 7, where the

integration time is 100 μs. Furthermore, in order to check the coherence of two channels, 250 measurements were conducted with a period of 5 minutes, and the peak phase of the result was extracted, as shown in Fig. 8. It is observed that, the peak phase difference has a mean value of -0.16 degree and a standard deviation of 2.50 degree for 250 measurements.

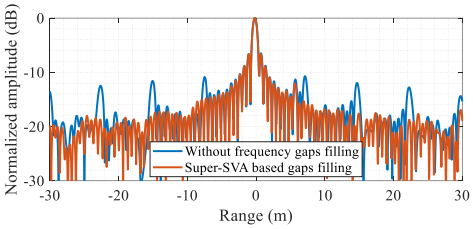

Fig. 7. Delay estimation result obtained by filling frequency gaps.

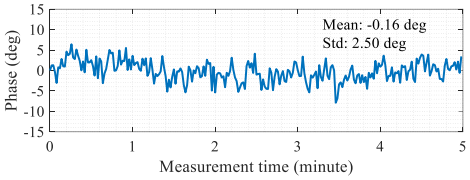

Fig. 8. Phase stability evaluation for 250 measurements.

Based on the aforementioned methodologies, passive bistatic SAR imaging experiments were carried out, as shown in Fig. 9, where the surveillance antenna is sled along a rail to detect a metallic plate. The moving step was 5 mm and the total sledding length was 1.2 m. The range compression results for each surveillance antenna position and the SAR image obtained by the BP algorithm are shown in Fig. 10. As we can see, the metallic plate can be well detected and focused.

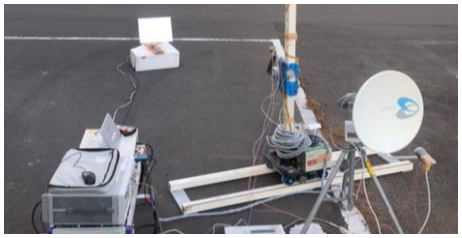

Fig. 9. SAR imaging of a stationary metalli plate.

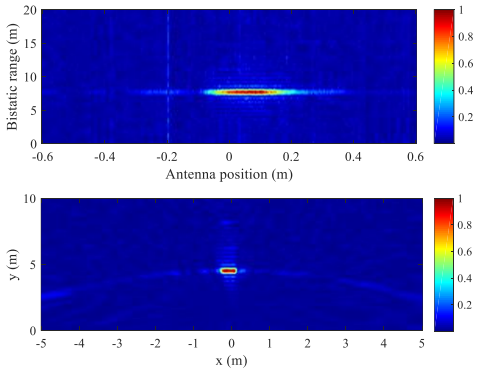

Fig. 10. Top: Range compression results. Bottom: SAR image.

At last, the displacement of the metallic plate, which was moved on a rail from 1 mm to 15 mm with a 1-mm step, was estimated. The acquisition time of each SAR image was about 45 seconds. The estimation results are shown in Fig. 11. It can be seen that the displacement of the metallic plate can be accurately estimated. The root mean square error (RMSE) of the estimation is about 0.27 mm.

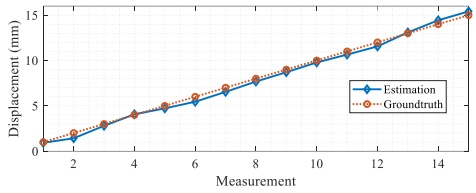

Fig. 11. Displacement estimation result.

VI. Conclusion

In this study, we developed a passive bistatic radar system using geostationary satellite TV signal with commercial-off-the-shelf hardware. LNB synchronization was used to increase the coherence for the long-time measurement and thus increase the SNR and the detection range. High range resolution was obtained by combing multiple TV channels. The artifacts caused by frequency gaps among different TV channels were reduced by means of a super-SVA based method. High azimuth resolution was achieved by moving the surveillance antenna on a rail to generate a synthetic aperture. Focused SAR images of targets were obtained by the back projection algorithm with reasonable approximations. Displacement of the target in the scene was estimated by the differential interferometric process. Compared to current GB-SAR system used for displacement estimation, the developed system is cheaper as it is does not need a transmitting unit. Multiple-direction displacement estimations can be obtained with multiple receivers using different bistatic geometries. Further work will be devoted to the generation of a DEM of the study area using an additional surveillance antenna. Multi-polarization capacity provided by the BS TV signal is also worthy to be studied. The potential applications of the developed system includes the continuous monitoring of landslides, buildings and dams.

Acknowledgements

This work was supported by JSPS Grant-in-Aid for Scientific Research (A) 26249058. The passive radar investigation is partly supported by the French Centre National de la Recherche Scientifique (CNRS) PEPS grant.

References

[1] H. D. Griffiths and C. J. Baker, “An introduction to passive radar,” Artech House, 2017.

[2] D. Gromek, K. Kulpa, and P. Samczynski, “Experimental results of passive SAR imaging using DVB-T illuminators of opportunity,” *IEEE Geosci. Remote Sens. Lett.*, vol. 13, no. 8, pp. 1124-1128, Aug. 2016.

[3] G. Nico, G. Cifarelli, G. Miccoli, F. Soccodato, W. Feng, M. Sato, S. Miliziano, and M. Marini, “Measurement of pier deformation patterns by ground-based SAR interferometry: Application to a bollard pull trial,” *IEEE J. Ocean. Eng.*, vol.43, no. 4, pp. 822-829, 2018.

[4] W. Feng, G. Nico, and M. Sato, “GB-SAR interferometry based on dimension-reduced compressive sensing and multiple measurement vectors model,” *IEEE Geosci. Remote Sens. Lett.*, vol. 16, no. 1, pp. 70-74, 2019.

[5] W. Feng, J. M. Friedt, and M. Sato, “Passive radar imaging by filling gaps between ISDB digital TV channels,” *IEEE J. Sel. Topics Appl. Earth Observ. Remote Sens.*, in press.